DISCLAIMER

CCD riddle: a) signal vs time: linear; b) signal vs variance: non-linear

Mark Downing[a], Dietrich Baade[a], Peter Sinclaire[b], Sebastian Deiries[a], Fabrice Christen [c].

[a]European Southern Observatory, Karl-Schwarzschild-Strasse 2, 85748 Garching Munich, Germany;
[b]ESO La Silla Observatory, Casilla 19001 Santiago 19, Chile;
[c]Kapteyn Astronomical Institute, Postbus 800, 9700 AV Groningen, The Netherlands.

ABSTRACT

Photon transfer curve is one of the most valuable tools for calibrating, characterizing, and optimizing the performance of CCDs. Its primary purpose is to determine the conversion gain of the CCD system, from which many of the other performance parameters such as read noise, dark current, QE, full well etc. are determined. Recent measurements on CCDs from different manufacturers have revealed that the photon transfer curve is non-linear (in excess of 15%) with the variance progressively becoming less at high signal levels than that predicted by simple photon shot noise. The puzzling thing is that the signal linearity is excellent and unaffected. This paper reports on the investigation which has isolated the source of the non-linearity to the CCD image area. Additionally, spatial autocorrelation analysis shows that the mechanism behind the non-linearity is due to spreading or sharing of charge between pixels in the image area. The authors only have a description of the phenomenon and invite all to help with an explanation.

Keywords: CCD, Photon Transfer Curve, CCD Characterization, autocorrelation, conversion gain.

1. INTRODUCTION

The photon transfer curve (PTC) is one of the most widely used techniques to determine the end-to-end conversion gain (e/ADU) of a CCD system. As it is simple to use (only requires the taking of pairs of flats in a progressive time series of constant illumination) and does not require complicated or specialized equipment, it is widely used at the telescope to check the health of the CCD and the CCD detector system. Most other parameters such as read noise, dark current, quantum efficiency (QE), full well are determined using this conversion gain.

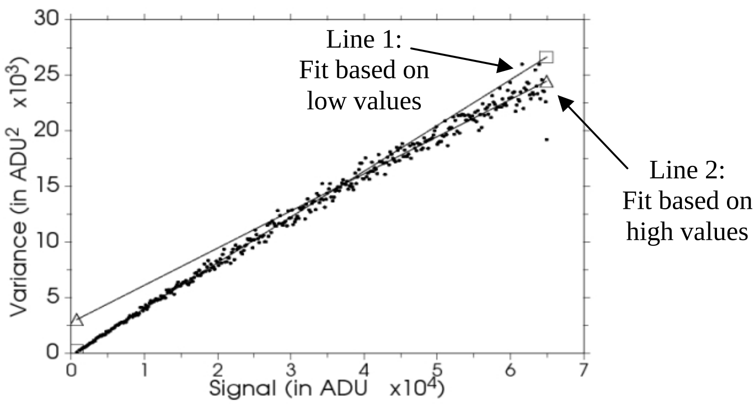

Fig. 1: Photon transfer curve (variance versus mean signal) of one of the OmegaCAM e2v CCD44-82 CCD provided by Fabrice Christen clearly showing the non-linearity. Line 1 is a linear fit based on the lower half (< 32,000 ADU) of signal data. Line 2 is linear fit based on the upper half (> 32,000 ADU) of signal data.

During the upgrade (completed April 2002) of the red arm of EMMI on the NTT telescope at La Silla Paranal observatories to a 2x1 mosaic of MIT/LL 2kx4k CCID-20 CCDs, Peter Sinclaire reported observing non-linearity in the Photon Transfer Curve during CCD characterization. Unfortunately due to pressure to complete the upgrade only a limited investigation was carried out at that time, but remained an interest to Sinclaire in the background. The non-linearity in the Photon Transfer Curve appears in the quality control (QC) data of La Silla Paranal observatories and this has been a concern for some time. Fabrice Christen[1] observed the non-linearity in the OmegaCAM e2v CCD44-82[5] CCDs.

Fig. 1 (provided by Christen) is a plot of the Photon Transfer Curve (variance versus unbiased signal) of one of the OmegaCAM CCDs where the non-linearity is clearly visible. Line 1 is a straight line fit to the lower half (< 32000ADU) of the signal data while Line 2 is a straight line fit to the upper half (>32000ADU). The most likely explanation of this type of non-linearity would be poor signal linearity; however this was not the case as excellent signal linearity was measured. This is puzzling as the literature says, and we have previously been taught that the photon transfer curve of CCDs should be linear. This must mean that there is something wrong and there is a need to investigate.

While several CCDs from two different manufacturers, e2v and MIT/LL, were tested, only the results of CCDs, e2v CCD44-82-1-952 serial number 27172-17-2 and 02395-04-01 respectively called Marlene and Pisces Australis II, and MIT/LL CCID-20 phase 3 CCD, serial number 14-4-6 called Catherine, are presented here. Both CCDs have 15 µm square pixels. The CCD44-82 CCDs are standard silicon 16 µm thick devices. The MIT/LL CCID-20 is a 40 µm thick high resistivity deep depletion CCD. The problem is not specific to a manufacturer or architecture as it has been observed on other manufacturers (Loral Lesser and TEK) CCDs, but to a much lesser extent.

2. MEASUREMENT TECHNIQUE AND INITIAL ASSESSMENT

The measurements were performed on the ESO ODT Test Bench[2] which has an excellent uniform flat field (~ 1% over 10cm x 10cm area) and stability of illumination to enable these tests to be easily carried out to a high degree of accuracy.

The photon transfer, calculated gain, and signal linearity curves were determined the standard way by taking a progressive increasing time series of two flats at constant illumination. The dark current of the CCDs were sufficiently low (< 2e/pix./hr.) to be ignored in the calculations. The residual signal non-linearity, *LR*, was calculated using the standard equation[3]:

$$LR = 100\left(1 - \frac{\overline{S_M}/t_{EM}}{\overline{S}/t_E}\right)$$

The variables $\overline{S}$ and t_E being the unbiased median signal and exposure time for each set of flats and $\overline{S_M}$ and t_{EM} are values chosen to provide mid-scale in the plot. The median signal, $\overline{S}$, the variance, *Var*, and the conversion gain, *Gain*, of the two flat fields, FF_1 and FF_2, and the two biases, B_1 and B_2, were calculated the standard way by:

$$FF_{diff} = FF_1 - FF_2$$

$$B_{diff} = B_1 - B_2$$

$$\overline{S} = \frac{\left(\overline{FF_1} + \overline{FF_2}\right) - \left(\overline{B_1} + \overline{B_2}\right)}{2}$$

$$Var = \frac{Var_{FF_{diff}} - Var_{B_{diff}}}{2}$$

$$Gain = \frac{\overline{S}}{Var} = \frac{\left(\overline{FF_1} + \overline{FF_2}\right) - \left(\overline{B_1} + \overline{B_2}\right)}{Var_{FF_{diff}} - Var_{B_{diff}}}$$

An initial assessment of the non-linearity was performed by analyzing images taken from MIT/LL Catherine and e2v Pisces Australis II. The results are shown in

Fig. 2. The top two graphs show linearity. The linearity of e2v Pisces Australis II is excellent with both amplifiers having signal non-linearity under ± 0.2%. The linearity of MIT/LL Catherine is not as good. The degradation of linearity of Catherine above 30,000 ADU (54 ke-) was diagnosed to be due to preamplifier saturation. However, linearity below this value is very good. The excellent signal linearity also demonstrates that the ESO Test Bench performs very well with respect to shutter timing and constancy of illumination. The photon transfer curve (bottom left graph) and especially the slope of the photon transfer curve, the calculated gain, versus signal (bottom right graph) show that the calculated gain is not constant, but varies with signal by up to 15%. The calculated gain varies continuously from low to high signal levels even though the CCDs are operated well below specified full well depth of 120 ke- (e2v) and 110 ke- (MIT/LL). The true conversion gain of the system is however constant as demonstrated by the excellent signal linearity so the explanation must be that the variance progressively becomes less at high signal levels than that predicted by simple photon shot noise.

As the graph of calculated gain versus signal (bottom right graph) shows the non-linearity superbly, it was used throughout the investigation to highlight the non-linearity.

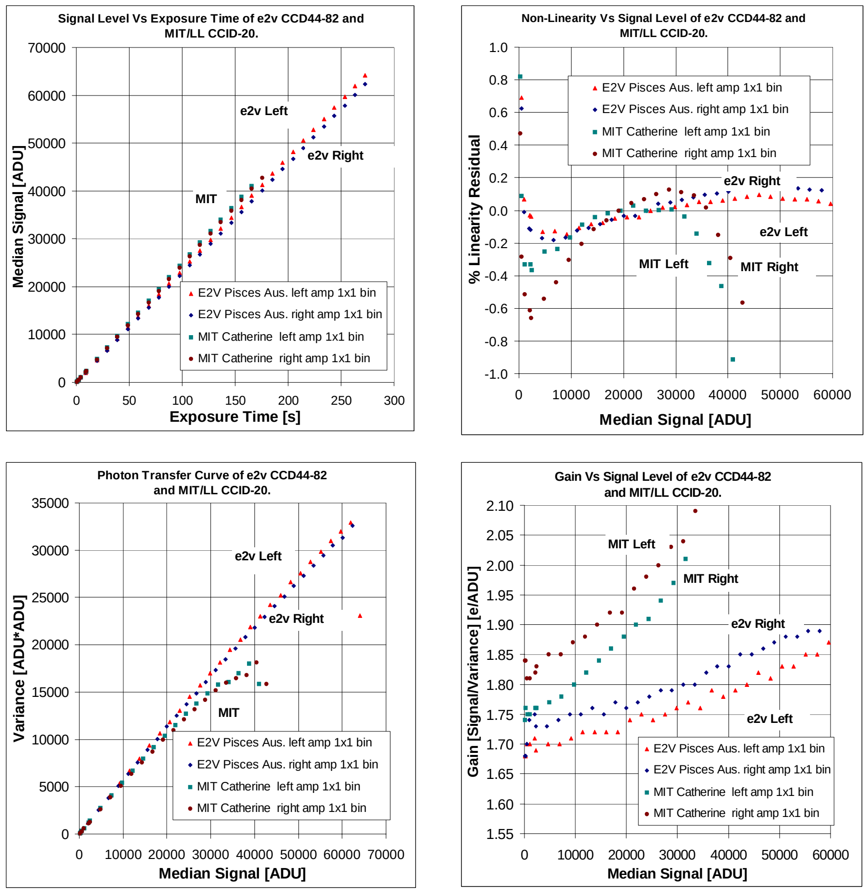

Fig. 2: Signal linearity and photon transfer curves of the left and right amplifiers of MIT/LL Catherine and e2v Pisces Australis II. Top Left: Signal versus exposure time; Top Right: Residual linearity curve; Bottom Left: Photon transfer curve (Variance versus Median Signal); Bottom Right: Calculated gain versus signal.

3. TESTS AND MEASUREMENTS PERFORMED TO LOCATE THE CAUSE

This section describes the investigation to isolate the non-linearity to a particular part of the CCD. This was performed by the technique of “divide-and-conquer”.

The first test was to determine whether the PTC non-linearity is due to something that happens in the image area or due to something in the serial register, output amplifier, or down stream controller electronics. Images were taken with different binning factors of x1, x2, x4, and x8 in the image area. By binning, the signal in the image area is kept low while the rest of the signal chain is exercised to high signal levels. The way this divides the problem is shown in the diagram of the CCD in the left of

Fig. 3. The plot in the right of

Fig. 3 shows the results. Clearly the non-linearity decreases substantially (calculated gain curve flattens) when the image area is binned and the signal is kept low in the image area. On the other hand, the serial register, the output amplifier, and the down stream controller electronics are exercised to the same high signal levels. At x8 binning in the image area, the calculated gain is essentially constant and does not vary with signal. The conclusion is that the PTC non-linearity is due to something that happens in the image area and has little to do with the serial register, output amplifier, and detector controller electronics.

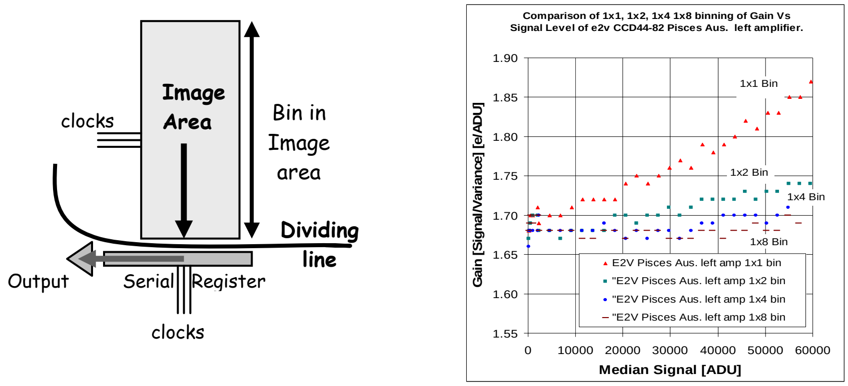

Fig. 3: Left: Diagram of CCD showing how binning of the image area divides the problem between the image area and the serial register, output amplifier, and down stream electronics. Right: Result of analysis showing calculated gain versus signal for binning factors of x1, x2, x4, and x8 in the image area. At higher binning factors (x8), the calculated gain is essentially constant and does not vary with signal thus the PTC non-linearity is due to something that happens in the image area.

Another possible explanation of the non-linearity is the manner in which the image area is clocked or the charge is transferred in the image area. To determine if either of these is responsible for the PTC non-linearity, the analysis was repeated on three regions of different clocking distances from the serial register; a region close to the serial register, a region in middle of the CCD, and a region at the top (farthest away from the serial register) of the CCD. The three regions are clocked a different number of times during the readout. The positions on the CCD of the regions selected are shown in the diagram in the left of

Fig. 4. The results (right graph of

Fig. 4) show that the PTC non-linearity varies little with the number of times the image area is clocked. As the image area charge transfer efficiency, CTE, of e2v Pisces Australis II has been measured to be very high at 99.9998% (by both ESO and e2v), the conclusion is that the PTC non-linearity is not due to the clocks or clocking of charge in the image area.

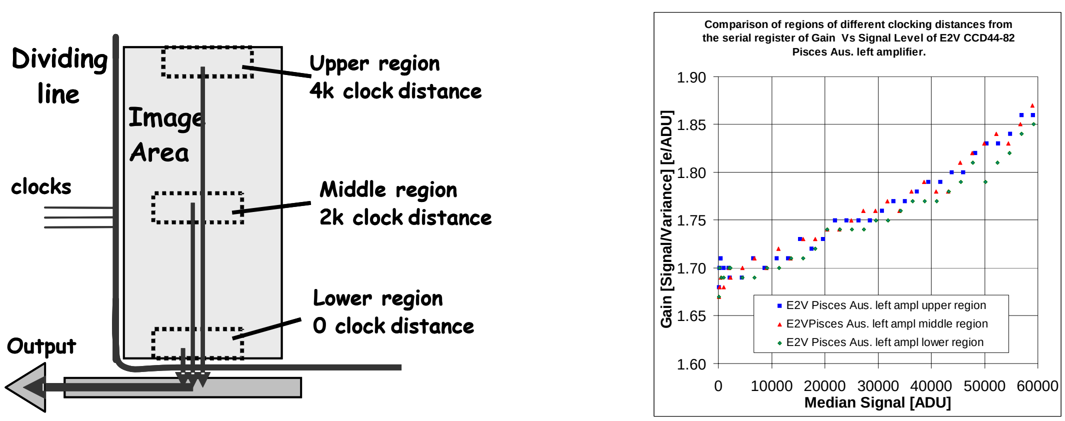

Fig. 4: Analyzing of three regions at different clocking distances from the serial register. Left: Diagram of CCD showing the regions selected; Right: Result of analysis showing calculated gain versus signal for the three regions. The PTC non-linearity varies little with the number of times the image area is clocked thus the non-linearity is not due to the clocks or clocking of charge in the image area.

The next area investigated was whether the non-linearity is due to charge generation or collection. The probability, P, of a photon being absorbed in silicon can be described by:

$$P = P_o e^{\left(-x_{EPI}/L_A\right)}$$

The probability is always a maximum, Po, at the silicon surface and then decreases with increasing depth, x_{EPI}, into the silicon. The absorption length, L_A, is the depth at which the probability has fallen to 1/e times the surface value. Using illumination of different wavelengths, it is possible to test whether the lateral diffusion of charge especially in the region at the backside of the CCD, where the electric fields of the clocks do not reach and remain undepleted, affect the non-linearity. Wavelength of illumination was varied from 400 to 900nm.

Fig. 5 (left side) shows a cross-section of a CCD depicting how shorter wavelengths have a higher probability of being absorbed near the silicon surface (the backside) than longer wavelengths.

Fig. 5 (right side) contains a table of the silicon absorption depths for the wavelengths tested.

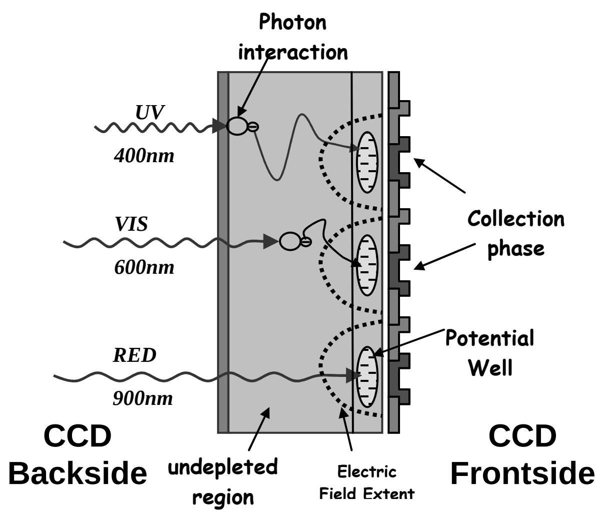

Wavelength (nm)	Absorption depth (µm)
400	0.2
500	1.0
632	2.7
700	4.8
800	10.5
900	28.6

Fig. 5: Light of different wavelengths is absorbed at varying depths in the silicon. Left: Cross-section of a CCD showing how photons of different wavelengths are absorbed at varying depths in the silicon. Right: Table of photon absorption depths in silicon as a function of wavelength.

Fig. 6 contains the results of the investigation. The right graph shows that the calculated gain varies little with the wavelength of illumination and thus it can be concluded that the non-linearity has little to do with lateral diffusion of charge in the undepleted region of the CCD. The left graph is the plot of mean signal versus exposure time for light of wavelengths 400, 500, 632, 700, 800, and 900nm. As the exposure time had to be adjusted to compensate for variation in the quantum efficiency of the CCD for different wavelengths, another result can be inferred from these measurements: the non-linearity is not highly dependent on the exposure time.

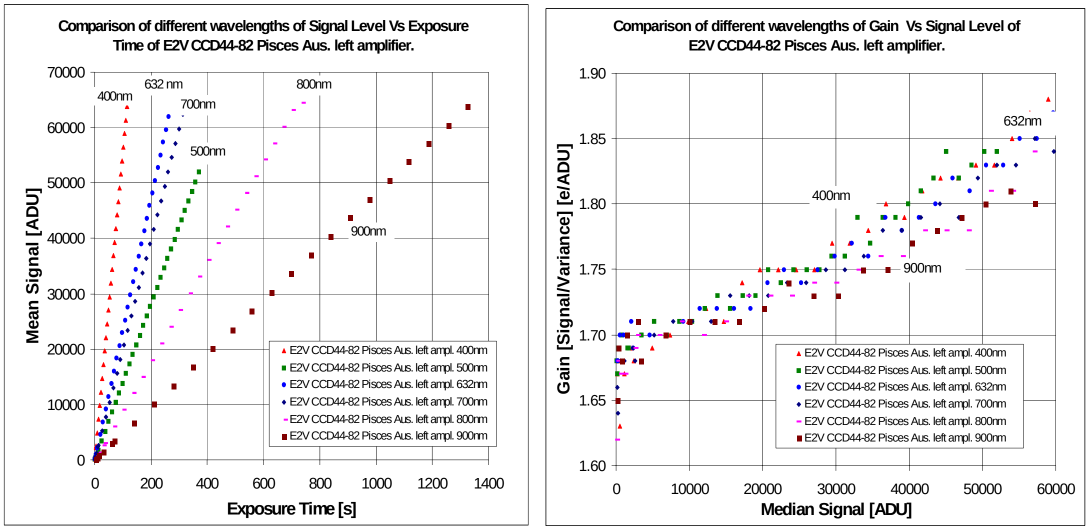

Fig. 6: Wavelength of illumination was varied to determine whether lateral diffusion of charge in the undepleted region at the backside of the CCD affected the non-linearity. Left: Plot of mean signal versus exposure time for light of wavelengths 400, 500, 632, 700, 800, and 900nm. Right: Result of analysis showing calculated gain versus signal for light of different wavelengths. The calculated gain varies little with the wavelength of illumination and thus the non-linearity has little to do with lateral diffusion of charge in the undepleted region of the CCD.

To determine if the settings of the image area clocks influenced the PTC non-linearity, the following tests were performed:

1. The low voltage levels of the image area clocks were varied from -8V to -9.5V and -6.5V to test if changing the operation of the image area from inversion (-9.5V) to non-inversion (-6.5V) affected the non-linearity.

The high voltage levels of the image area clocks were varied from +2V to +1V and +3.5V. This changes the extent of the electric fields (see CCD cross-section in

2. Fig. 7) generated by the image area collecting phase and thus the depth of the undepleted region at the backside of the CCD.

3. The number of clock phases left high during the exposure were varied from one to two. As in 0 above, the extent of the electric field generated by the clocks increases with the number of phases left high and thus reduces the depth of the undepleted region at the backside of the CCD.

The results are shown in the right of

Fig. 7. The results show that the PTC non-linearity varies little with changes in the voltages of the image area clocks or with the number of clock phases left high during the time photons are collected. From these measurements, the following conclusions can be made. The PTC non-linearity has little to do with:

1. whether the image area is run inverted or not.
2. the lateral diffusion of charge in the undepleted region of the CCD; confirming a previous conclusion.

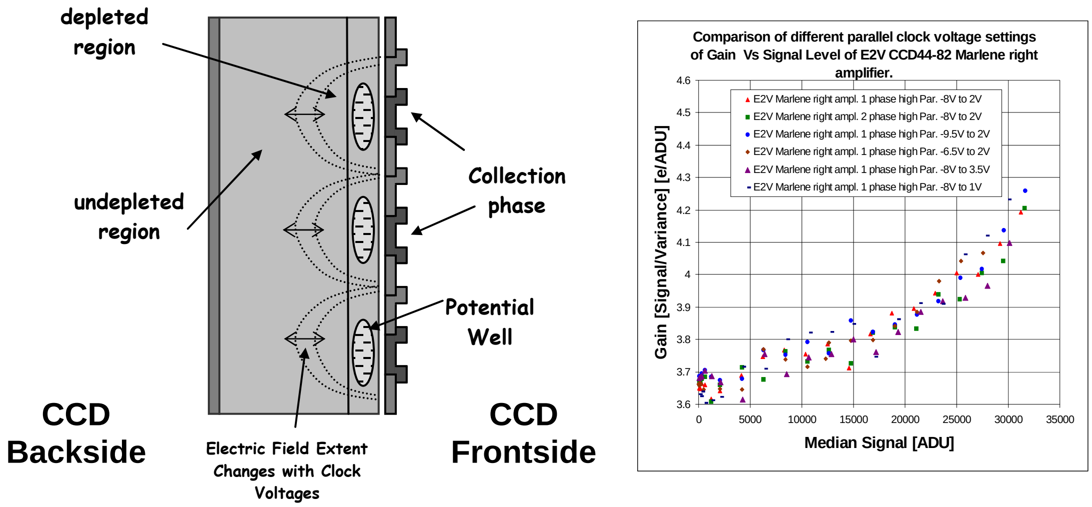

Fig. 7: Image area clock voltages and the number of phases kept high during the time photons are collected were varied. Left: Diagram of CCD showing how the extent of the electric field changes with the clock voltage setting. Right: Results of analysis showing calculated gain versus signal for various voltage settings. Results show that the PTC non-linearity varies little with change in voltages of the image area clocks or with the number of clock phases left high during the time photons are collected.

The operating temperature (-120°C and -80°C) of the CCD was varied to determine if this influenced the PTC non-linearity. The results are shown in Fig. 8. The gain of the output amplifier of the CCD changes with temperature as expected, but the shape of the curve essentially remains the same. The conclusion is that the non-linearity of the PTC has little dependency with temperature.

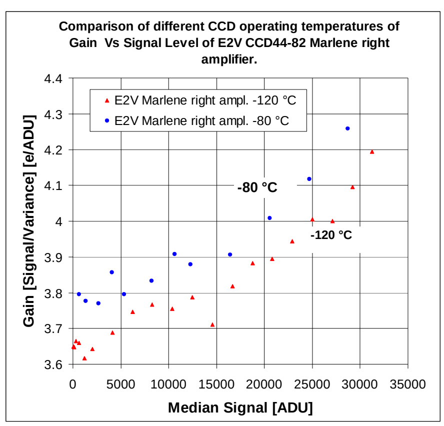

Fig. 8: Results of analysis showing calculated gain versus signal for CCD temperatures of -120°C and -80°C. Shape of the curve essentially remains the same thus PTC non-linearity has little dependency with temperature.

4. SPATIAL AUTOCORRELATION ANALYSIS

To determine if the observed reduction in variance with signal level is due to an interaction (spreading) of charge between neighboring pixels (i.e. some type of signal smoothing over pixels), the 2D spatial autocorrelation function $R_{m,n}$ of pixel (m,n) was calculated by taking the difference, $V_{i,j}$, of two uniformly illuminated shot noise limited images (size MxN) and using the autocorrelation equation:

$$R_{m,n} = \frac{\sum_{i=1,j=1}^{i=M-m,j=N-n} V_{i,j} V_{i+m,j+n}}{\sum_{i=1,j=1}^{i=M,j=N} V^2_{i,j}}$$

Note that if the signals of neighboring pixels are not correlated, then the sum of the cross products $V_{i,j}V_{i+m,j+n}$ (i.e. where $m \neq 0$ and $n \neq 0$) should be 0 and $R_{m,n}$ = 0 where $m \neq n$ and $R_{m,n}$ = 1 where $m = n$. Gert Finger[4] has recently performed this type of analysis on CMOS Hybrid detectors from Rockwell and Raytheon and reported finding correlation between pixels on these detectors.

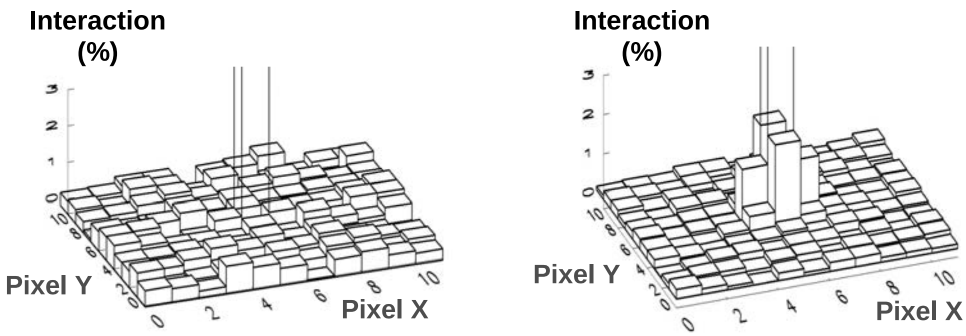

Fig. 9: Results of 2D spatial autocorrelation analysis of data taken with e2v Pisces Australis II. Left: Pixel interaction plot of ~ 88 ke- flat field images where the image has been binned x8 in the image area. No correlation is seen between pixels. Right: Pixel interaction plot of ~ 90 ke- flat field images where no binning has been performed. Correlation is clearly visible.

Fig. 9 shows the result of the 2D spatial autocorrelation analysis. The left plot of Fig. 9 is the result of analysis of two 88 ke- flat field images which have been binned on-chip by 8 in the image area. The central pixel is off-scale and is of value ~ 100%. No correlation is seen between pixels. This is as expected because when the image is binned in the image area, the serial register, output amplifier, and down stream electronics are exercised to high signal level but the signal in the image area remains low (11 ke-) and very little non-linearity in the PTC is seen. Please refer to

Fig. 3 and the accompanying text which discusses this in detail.

On the other hand, the right plot of Fig. 9 is the results of analysis for two 90 ke- flat field images which are not binned. Correlation is clearly visible. In this case, the signal in the image area is high and considerable amount of non-linearity of ~ 10% is seen in the photon transfer curve (refer to

Fig. 2).

Note the difference in correlation between pixels in the horizontal (1.4%) and vertical (2.2%) directions. This indicates that the mechanism behind the interaction of pixels is dependent on the different structure (see left diagram of Fig. 10) of the CCD in the horizontal (pixel defined by the channel stop) and vertical (pixels defined by the electric fields created by the clock lines) directions. This difference is understandable and somewhat expected.

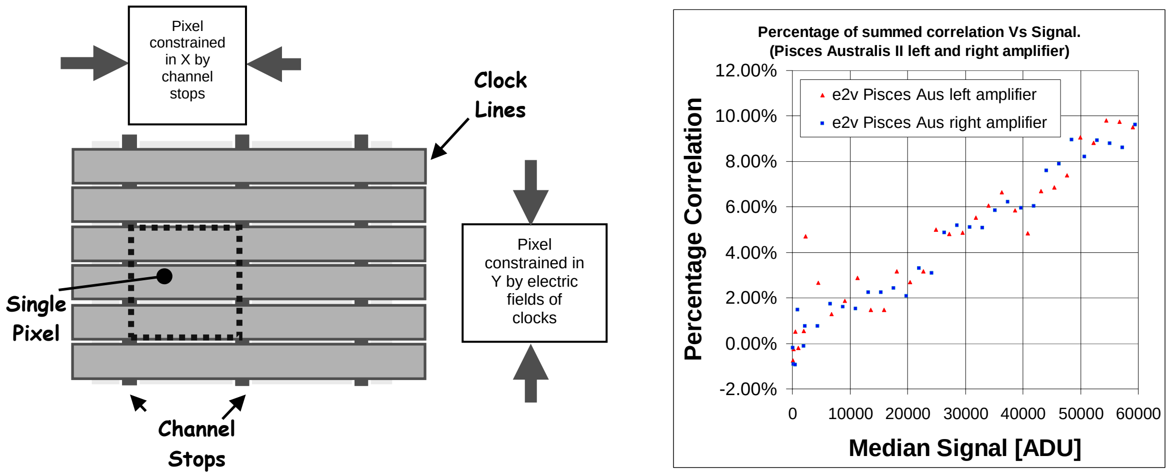

Fig. 10 : Left: Top view of CCD showing the different structure of the CCD in the horizontal (pixel defined by the channel stop) and vertical (pixels defined by the electric fields created by the clock lines) directions. Right: Plot of summed total correlation between pixels versus signal level in the image area of the left and right amplifiers of Pisces Australis II.

The correlation between adjacent pixels is small at 1.4 to 2.2%. However, the summed correlation of all neighboring pixels is 10% which is significant as it results in over estimating the gain of the system by 10%. The plot (right of Fig. 10) of the summed correlation of all neighboring pixels for a given pixel, for different signal levels shows that the correlation between pixels increases continuously from low to high signal level in the image area.

The autocorrelation variance, Var_{AC}, over an image area of M x N pixels can be calculated by the following equation,

$$Var_{AC} = \frac{\sum_{m=-P,n=-R}^{m=+P,n=+R} \sum_{i=1,j=1}^{i=M-m,j=N-n} V_{i,j} V_{i+m,j+n}}{(M.N-1)}$$

where the interaction between pixels is taken into account and is contained within pixel distance of P x R. If this autocorrelation variance is used instead of the normal form of the variance,

$$Var = \frac{\sum_{i=1,j=1}^{i=M,j=N} V^2{}_{i,j}}{(M.N-1)}$$

the conversion gain, $Gain_{AC}$, by autocorrelation of the CCD system can be calculated as follows:

$$Gain_{AC} = \frac{\bar{S}}{Var_{AC}}$$

where $\bar{S}$ is the mean unbiased signal. The left plot in Fig. 11 compares the conversion gain of the left amplifier of Pisces Australis II calculated by both the normal and the autocorrelation variance for different signal levels. The gain calculated by autocorrelation is independent of the signal level and agrees extremely well with the results of the gain calculated in

Fig. 3 when the signal is kept low (very little non-linearity in the PTC) in the image area by binning by 8.

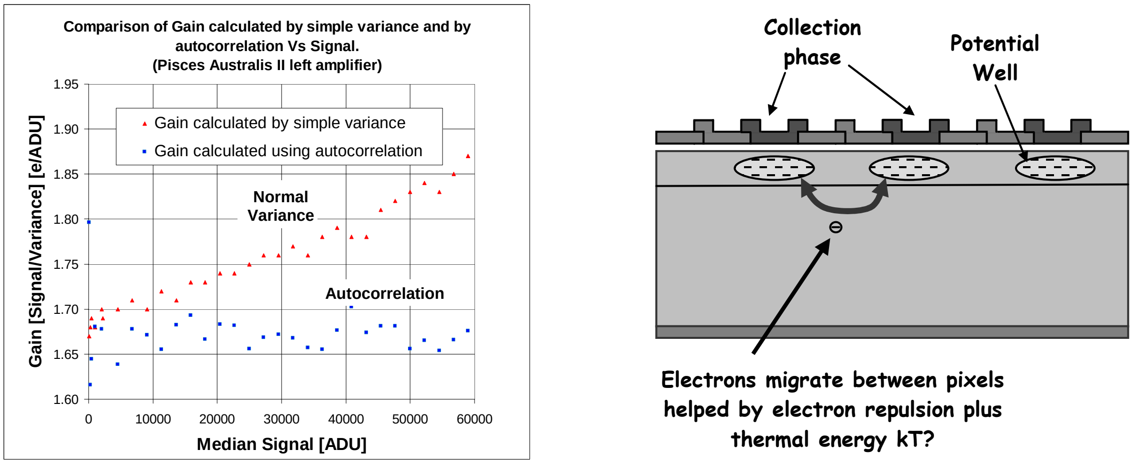

Fig. 11 : Left: Plots of calculated gain versus signal level of the left amplifier of Pisces Australis II. In the top graph is gain calculated by the simple variance. In the bottom graph gain is calculated by the autocorrelation variance. The autocorrelation gain is independent of the signal level and is the correct conversion gain. Right: Cross-section of the CCD providing simple explanation of how electrons migrate between the potential wells of the pixels.

A possible simple explanation of this interaction (charge sharing or spreading) between neighboring pixels is that the charge collected in the potential well of the pixel somehow migrates (diffuse) to their neighbors. The likelihood of this migration occurring is increased by the mutual electrostatic repulsion force of electrons. The more charge in a potential well, the greater the repulsion force and the greater chance of migration. This process could be assisted by thermal diffusion (*kT* energy). This explanation is show graphically in the right of Fig. 11. The evidence does not fully support this explanation as the number of migrated electrons should increase with time and be dependent on temperature. This has not been observed (refer to Fig. 6 and Fig. 9 and accompanying text). In addition, the thermal energy (*kT*) is about 0.015 eV at -120 °C and the probability of surmounting a potential barrier even as low as 1 volt would be extremely low at ~ $e^{-V/kT} = e^{-66}$.

5. EFFECT ON THE APPLICATION

This investigation would not be complete without discussing the effect on the end application; the acquisition of images in imaging and spectroscopic instruments on optical telescopes. For this application our major area of concern is on the calibration of scientific data and spatial performance (i.e. Point Spread Function, PSF) of the CCD.

The effect on calibration of scientific data is minimal. Bias frames are unaffected. The signal linearity is good and there is no loss of charge. Flat fielding is therefore unaffected. The major effect is where the variance is used to determine CCD parameters. The major parameter is as expected the conversion gain. By using the following simple rules, the estimation of the gain can be improved significantly and is therefore not seen as a problem:

1. Calculate gains at low signal levels; just high enough for photon statistic noise to dominate over read noise, but low enough so that the interaction between pixels is small. A good rule of thumb in past is to use signal levels of ~ 10,000e.
2. Bin charge to keep signal low in the image area. Binning by 8 in the image area is best.
3. For the greatest accuracy, use the autocorrelation variance (section 4) to calculate the gain.

A feel for how the correlation between pixels influences the spatial performance of a CCD can be obtained by examining measurements taken at ESO by Cyril Cavadore where a small spot of light (3-5 µm) was shone into the middle of a pixel. See the diagram in the left of Fig. 12 that describes the technique. An estimation of the spatial performance of the

CCD can be obtained by calculating the percentage of light in the target pixel compared to the total illumination of all pixels as follows:

$$Pixel\ Percentage\ = \frac{Signal\ in\ Central\ Pixel}{Total\ Signal\ of\ Region\ affected\ by\ Illumination}$$

A *PixelPercentage* of 100% means that 100% of the light shone into the pixel is collected by that pixel. A plot of *PixelPercentage* versus different wavelength for an e2v standard silicon CCD44-82 and a MIT/LL 40 µm high resistivity CCID-20 CCDs is shown in the right of Fig. 12. On this plot, arrows of 15% height have been placed. These are equivalent to the correlation between pixels seen at high signal level. Clearly the correlation between pixels has a noticeable effect on the spatial performance of the CCDs and this influence is greater at longer wavelength where the lateral diffusion of charge in the undepleted region is less dominant. The signal level at which these measurements were performed and thus the exact amount of correlation between pixels is unknown. This is an area of future research where these measurements will be repeated at varying illumination levels to try and separate the correlation between pixels from other items that influence spatial performance such as lateral diffusion of charge in the undepleted region.

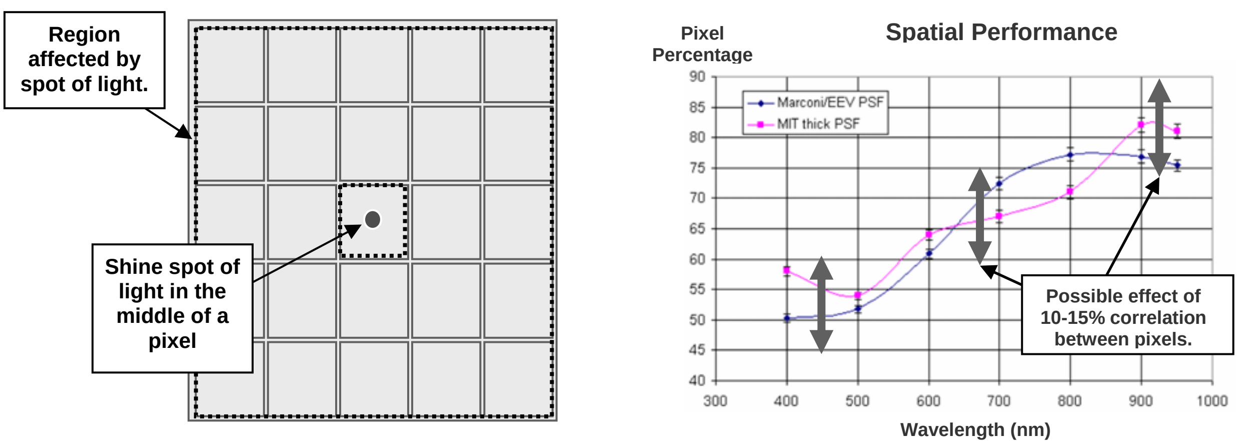

Fig. 12: Left: Diagram showing the technique used to obtain an estimate of the spatial performance of CCDs. A spot of light is shone in the middle of a pixel and the ratio of signal in this pixel is compared to the total of all pixels. Right: Plots of percentage of light collected in the middle pixel versus wavelength.

6. CONCLUSION

An investigation was carried to locate the cause of the non-linearity observed in the Photon Transfer Curve. Tests show that the non-linearity is due to the level of charge in the image area and is not due to the image area clocks, lateral diffusion of charge in the undepleted region at the back of the CCD, serial register, output amplifier, or detector electronics. Spatial autocorrelation analysis showed that the mechanism behind the non-linearity is due to spreading or sharing of charge between the potential wells of the pixels in the image area and this interaction progressively increases with signal level. In addition, it was shown that the conversion gain can be correctly calculated by using the autocorrelation variance rather than the normal form of the variance. If the traditional method is used, then the use of binned pixels and low image area signal levels is recommended.

A simple explanation of electrons migrating between potential wells was proposed to explain the interaction between neighboring pixels. This migration is a result of some sort of (thermal?) diffusion where the probability of occurrence is increased by the greater mutual electrostatic repulsion force between electrons as electrons build up in the potential well. The evidence does not fully support this explanation and the authors invite all to help with a more accurate explanation.

The effect on calibration of scientific data and spatial performance of the CCD was discussed. The effect on calibration of the scientific data is believed to be minimal except one has to be careful in calculating the conversion gain. On the other hand, the spatial performance of the CCD is affected and follow up work is proposed to investigate this further in the future and to separate pixel correlation from other items that influence spatial performance such as lateral diffusion of charge in the undepleted region.

Some simple rules were provided to more accurately use the Photon Transfer Curve to calculate the conversion gain. This leads to the conclusion that the use of the Photon Transfer Curve should not be abandoned, but care exercised in its use.

7. ACKNOWLEDGEMENTS

The authors wish to thank G. Finger for his enlightening discussions and helpful suggestions.

REFERENCES

1. F. Christen et al, "Fast conversion factor (gain) measurement of a CCD using images with vertical gradient", Scientific Detectors for Astronomy 2005, pp. 537-542, June 2005.
2. http://www.eso.org/projects/odt/CCDtestbench/index.html.
3. J. Janesick, "Scientific Charge-Coupled Devices", SPIE PRESS Vol. PM83, pp. 117-120, January 2001.
4. G. Finger et al, "Conversion gain and interpixel capacitance of CMOS hybrid focal plane arrays", Scientific Detectors for Astronomy 2005, pp. 477-490, June 2005.
5. e2v technologies, "CCD44-82 Data Sheet", Document number A1A-CCD44-82_BI, June 2004.